Comparative analysis of the toxicity of gold nanoparticles in zebrafish

Patibandla, Srinath; Zhang, Yinan; Tohari, Ali Mohammad; Gu, Peng; Reilly, James; Chen, Yu; Shu, Xinhua

Published in:
Journal of Applied Toxicology

DOI:
10.1002/jat.3628

Publication date:
2018

Document Version
Peer reviewed version

Comparative analysis of the toxicity of gold nanoparticles in zebrafish

Srinath Patibandla[1], Yinan Zhang[2,3], Ali Mohammad Tohari[1,4], Peng Gu[2], James Reilly[1], Yu Chen[2], Xinhua Shu[1*]

1 Department of Life Sciences, Glasgow Caledonian University, Glasgow G4 0BA

2 Department of Physics, University of Strathclyde, Glasgow G4 0NG

3. College of Physics, Jilin University, Changchun, 130012, China

4 King Fahad Hospital, Jazan, Saudi Arabia P.O BOX 204

* Corresponding author Xinhua Shu, Email: Xinhua.Shu@gcu.ac.uk

Abstract

The use of nanoparticles - particles that range in size from 1 to 100 nanometres - has become increasingly prevalent in recent years, bringing with it a variety of potential toxic effects. Zebrafish embryos were exposed during the 3-day post-fertilisation period to gold nanospheres (GSSs), gold nanorods (GNRs), gold nanorods coated with polystyrene-sulfate (PSS-GNRs), and gold nanorods coated with both polystyrene-sulfate and polyallamine hydrochloride (PAH/PSS-GNRs). All nanorods were stabilised with cetyltrimethylammonium bromide (CTAB). GNSs were the least toxic of the nanoparticles studied, with exposure resulting in no significant changes in mortality, hatching or heart rate. Exposure to GNRs and PSS-GNRs resulted in significant increases in mortality and significant decreases in hatching and heart rate. Treatment with GNRs caused significant changes in the expression of a variety of oxidative stress genes. The toxic effects of GNRs were ameliorated by coating them with polystyrene-sulfate and, to a more marked extent, with a double coating of polystyrene-sulfate and polyallamine hydrochloride.

Keywords Nanoparticles; nanospheres; nanorods; zebrafish; toxicity

Short abstract

Zebrafish embryos were exposed during the 3-day post-fertilisation period to gold nanospheres (GSSs), gold nanorods (GNRs), and to gold nanorods coated with polystyrene-sulfate alone (PSS-GNRs) or in combination with polyallamine hydrochloride (PAH/PSS-GNRs). All nanorods were stabilised with cetyltrimethylammonium bromide. Exposure to GNSs had no significant effects, whereas exposure to GNRs and PSS-GNRs significantly affected hatching, heart rate and mortality. Exposure to GNRs caused significant changes in the expression of various oxidative stress genes. Coated nanorods had markedly less toxic effects.

1 INTRODUCTION

Particles ranging in size from 1 to 100 nanometres (nm) are known as nanoparticles; the use of such particles is known as nanotechnology. In the field of biology, engineered nanoparticles have been put to a variety of uses, including (to mention only a few examples): as fluorescent biological labels, in the diagnosis, monitoring and destruction of tumours, in detection of pathogens and proteins, in gene expression and phagokinetic studies, and in MRI contrast enhancement (Salata, 2004; Zhang et al, 2010, 2011, 2015;). Carbon nanoparticles are widely used in vehicles and sports equipment. Cerium oxide is used in electronics, fuel additives and biomedical supplies, while titanium dioxide is widely employed in cosmetics, paints and coatings. Silver nanoparticles are used in the food and textile industries for their antimicrobial properties, while iron nanoparticles are used as smart fluids in the fields of optics and food supplement industries Gold nanoparticles have been used in drug delivery, tumour detection, gene therapy, and as photothermal agents (Asharani *et al.,* 2008; Wei, 2015, 2016).

The bio-distribution and bioactivity of nanoparticles, and the resulting human and environmental impact, are not well known, but their effects have been investigated in a variety of *in-vitro* and *in-vivo* studies. There is evidence that nanoparticles such as carbon, silver, iron, cerium and titanium oxides exhibit toxicological impacts on the environment (Asharani *et al.,* 2009). This potential toxicity has become a matter of concern. Some studies have reported a significant increase in inflammation markers in the airways, leakage of the blood-brain barrier, neuronal damage and cerebral oedema after exposure to nanoparticles (Cattaneo *et al*., 2014)**.** Zinc oxide nanoparticles show anti-microbial activity by damaging cell membranes and organelles and might cause the same kind of damage to eukaryotic cells (Marambio-Jones *et al.,* 2010). Zinc oxide nanoparticles can cause cytotoxicity in immune cells and cardiovascular damage (Wolf *et al*., 2015; Hanley *et al*., 2009). Reports show that

nanoparticles have a greater potential for damage compared to larger particles (Asharani *et al.,* 2008). Given the range of possible toxic effects, and the wide variety of nanoparticles implicated in these effects, more research is needed to identify the ways by which they disperse, their impact on organisms and on the environment, and how to minimise these effects.

One approach is to use the zebrafish animal model to assess toxicity caused by nanoparticles. The zebrafish is recognised as an alternative model by which to analyse human physiology, development and disease. It has been used widely because of its many benefits such as easy maintenance in labs, production of large number of optically transparent eggs, homology to the human genome, and rapid development of the embryo to adult fish by the end of week 1 post fertilisation. The zebrafish embryos are preferable because of their sensitivity to test chemicals and their ability to absorb test substances through their skin and gills from the surrounding water (Bar-Ilan *et al*., 2009). Transmission electron microscopy (TEM) and acridine orange staining have been used to investigate the distribution of nanoparticles (and the resulting cell death) in blood, brain and yolk sac in zebrafish embryos (Asharani *et al.*, 2008;).

2 MATERIALS AND METHODS

2.1 Nanoparticle syntheses and characterization

Gold nanospheres (GNSs) were prepared according to the Turkevich method (Kimling *et al.* 2006). Gold nanorods (GNRs) were synthesised by the seeded growth method (Murphy & Jana (2002). Typically, 2.5ml $HAuCl_4x3H_2O$ (0.001M) and 0.6ml ice-cold $NaBH_4$ (0.01M) were added to 7.5ml cetyltrimethylammonium bromide (CTAB) (0.12M) to prepare the seed solution. The growth solution was synthesized by adding 0.15M benzyldimethylhexadecylammonium chloride (BDAC), 50ml $HAuCl_4x3H_2O$ (0.001M), 3ml

silver nitrate ($AgNO_3$) (0.004M) and 700µl ascorbic acid (0.778M) to 50ml CTAB solution (0.1M). 80µl seed solution (2 hours after preparation) was then injected into the growth solution to grow gold nanorods. The nanorods could then be coated with a single layer of PSS or a double layer of PAH-PSS using the method described by Omura *et al*. (2009).

GNSs, GNRs and polymer coated GNRs sample solutions (quantity 3ml) were placed in a quartz cuvette and absorption spectroscopy studies carried out using a JASCO V-660 absorption spectrometer. The physical properties of the prepared gold nanoparticles were characterized using transmission electron microscopy (TEM).

2.2 Nanoparticle treatment

The zebrafish (*Danio rerio*) used in this study were obtained from our fish breeding stocks ZEBTEC zebrafish housing system (Tecniplast), Glasgow Caledonian University. Fish are kept in 5L plastic tanks supplied with a constant flow of conditioned water at a temperature of 28°C with pH 7.5 on a 14:10h light/dark photoperiod. Eggs were collected from a group of spawned zebrafish.

The embryos were exposed to GNSs, GNRs, PSS-GNRs or PAH/PSS-GNRs at concentrations of 0.01, 0.025, 0.05 and 0.1nM in a 48–well plate. To prepare the dilutions, each sample of nanoparticles was mixed with system water. For the negative control, system water alone was used. The collected eggs were bleached with chlorine water at a concentration of 5µl of 10-15% chlorine water in 17 ml of system water for 2 to 3 minutes to avoid any contamination and infection, then washed three times with fresh system water to remove any traces of chlorine. Within 2h post fertilisation (hpf), fertilised and normally developing fish eggs were transferred into each well (8 embryos/well) using a plastic pipette, then incubated at 28°C. The eggs were exposed to the test samples during the 3-days post-fertilisation period and inspected at 24, 48 and 72 hpf for mortality, hatching, morphological abnormalities, heart rate, body length and eye size.

Mortality of the embryos was noted at 24, 48 and 72 hours of nanoparticle treatment. The opaque and white embryos were transferred along with the medium to other empty wells and inspected in order to differentiate dead embryos (which quickly degrade) from abnormal or malformed embryos. The abnormal embryos were again transferred to their respective test wells. Mortality rate is expressed as the percentage of dead embryos after 72 hpf (hours post fertilisation). Hatching rate (expressed as the percentage of embryos that had hatched by 72 hpf) was recorded. Heart rate was monitored at 72 hpf using a stopwatch and direct microscopic observation. Tail detachment, the formation of somites, presence of brown flakes and any abnormalities were observed and noted.

2.3 Acridine orange staining

To investigate the cell death (apoptosis) caused by nanoparticles, acridine orange staining of nanoparticle-treated embryos was performed. Acridine orange is a nucleic-acid-selective metachromatic dye that emits green fluorescence upon intercalation with DNA and is widely used for detecting the sites of apoptosis in zebrafish. Acridine orange can permeate apoptotic cells and bind to DNA whereas normal healthy cells are non-permeable to acridine orange. Acridine orange staining was performed according to previous description (Shu et al., 2010). Briefly, the embryos were transferred to 1.5ml Eppendorf tubes and stained with acridine orange (5 µg/ml) for 20 min at room temperature. Embryos were washed quickly in 1×PBS and were observed using green fluorescence microscopy. The fluorescent signals from apoptotic cells (heart and eye areas) were quantified using ImageJ software (https://imagej.nih.gov/ij/). In brief, the heart and eye areas were selected using the selection tool, and the integrated density and mean gray value were measured. In each case, a nearby region with background fluorescence was selected for comparison, and the integrated density and mean gray value were measured for this region. Total fluorescent signals were calculated

using the formula: total fluorescent signals = integrated density - mean fluorescent signals of background.

2.4 RNA extraction

Zebrafish eggs were collected in a Petri dish and bleached with chlorine to prevent infections. At 6hpf embryos were treated with 4 nanoparticle samples (2.5 µM GNS, 0.01 nM GNR, 0.025 nM PSS-GNR and 0.05 nM PAH/PSS-GNR) till 72hpf with E3 medium as control. The treated zebrafish embryos were homogenised in 1 ml of TRIzol® Reagent (Invitrogen cat. no. 15596-026) per 50–100 mg of the tissue sample. Homogenised samples were incubated for 5 minutes at room temperature to allow complete dissociation of the nucleoprotein complex. 200 µl of 100% chloroform per 1 ml of TRIzol® Reagent used for homogenization was added to each sample. All samples were manually and vigorously shaken for 15 seconds and allowed to stand for 2-3 minutes at room temperature. All tubes were centrifuged at 12,000 × *g* for 15 minutes at 4°C. The resulted supernatant contains three aqueous layers in which RNA is found in the top layer. Each upper aqueous layer was transferred to a fresh 1.5 ml Eppendorf tube and 500 µl of 100% isopropanol per 1 mL of TRIzol® Reagent used for homogenization was added to the aqueous phase and allowed to stand for 10 minutes at room temperature. All tubes were then centrifuged at 12,000 × *g* for 10 minutes at 4°C. Supernatants were discarded by inverting the tubes leaving only the RNA pellet which was then washed by adding 75% ethanol. Following centrifugation the RNA pellet was allowed to stand for 5-10 minutes at room temperature to permit the evaporation of remaining traces of the ethanol wash. The RNA pellet was resuspended in 25 µl of RNase-free water and the purity was assessed using Nanodrop spectrophotometer (ND1000) in which RNA purity is defined as A260/280 ratio.

2.5 cDNA synthesis

Complementary DNA (cDNA) synthesis was performed using Roche Transcriptor High Fidelity cDNA Synthesis Kit (cat. no. 05091284001) according to the manufacturer's instructions. The protocol was carried out in 20µl reaction volume in two steps. First step: 4µl of neat RNA was incubated with 2µl of 600µM random hexamer primer and 5.4µl RNase-free water for 10 minutes at 65°C and the product was immediately chilled in ice. The second step involved addition of 8.6 µl of a master mix containing 4 µl of 5X transcriptor high fidelity reverse transcriptase reaction buffer, 0.5 µl of 40 U/µl Protector RNase inhibitor, 2 µl of 10 mM deoxynucleotide mix, 1 µl of 0.1M Dithiothreitol (DTT) and 1.1 µl of 100U/ µl of transcriptor high fidelity reverse transcriptase followed by brief centrifugation at 4°C. The cDNA reaction mixture was incubated in a thermal cycler for 10 minutes at 29°C followed by a second incubation for 60 minutes at 48°C and then final incubation for 5 minutes at 85°C to inactivate the transcriptor high fidelity reverse transcriptase. The resultant cDNA was then quantified using Nanodrop spectrophotometer (ND1000) and stored at -20°C.

2.6 Quantitative real-time PCR (qRT-PCR)

The expression of candidate oxidative stress genes following zebrafish microparticles treatment was analysed using Platinum® SYBR® Green qPCR SuperMix-UDG master mix (Invitrogen Cat 11733-046) according to the manufacturer's protocol in a final volume of 20µl containing 10 µl of Platinum® SYBR® Green qPCR mix, 7µl of PCR-grade water, 1µl of forward primer (10µM), 1µl of reverse primer (10µM), and 1µl of 50ng/ µl of cDNA. The primer sequences of target genes are listed in Table 1. The qRT-PCR reaction mixture was then assayed using the Biorad CFX96^{TM} Real-Time PCR detection system under the following PCR conditions: UDG incubation at 50°C for 2 minutes followed by Taq polymerase activation for at 95°C for 2 minutes and 40 cycles of 95°C for 15 seconds, 55°C for 30 seconds, and 72°C for 1 minute. Fluorescence signal detection was measured at 72°C.

198 The amount of mRNA is determined by normalizing the threshold cycle C_T of the candidate
199 gene to the C_T of ZF18sRNA reference gene in the same sample based on the following
200 formula: the average C_T of target gene - the average C_T of reference gene in which this result
201 is recognized as ΔC_T where it is specific for each gene and can be compared with ΔC_T of
202 calibration samples. The difference between ΔC_T of target and control genes is known as
203 $\Delta\Delta C_T$. The relative quantification of target gene expression is calculated in comparison with
204 control according to the following formula: $2^{-\Delta\Delta CT}$ and represented as a fold change.

205 **2.6 Statistical analysis**

206 All experiments were done at least in triplicate. Data were expressed as mean (±standard
207 error) and subjected to analysis of variance (ANOVA) followed by the Tukey's test. ANOVA
208 assumptions (normality and homogeneity of variances) were previously checked. The
209 significance level adopted was 95% (C= 0.05).

210 **3 RESULTS**

211 **3.1 Characteristics of nanoparticles**

212 The absorption spectra for GNRs, PSS-GNRs and GNSs are shown in Figure 1. As can be
213 seen, the surface plasmon of GNSs peaks at 525nm, while there are two peaks both for GNSs
214 and PSS-coated GNRs: one located around 525nm (which is referred to as the transverse
215 mode) and one in the near infra-red band (known as the longitudinal mode). The surface
216 plasmon structure depends critically on the particle size, shape and surface conditions. Figure
217 2 shows typical TEM images of gold nanospheres and gold nanorods of longitudinal surface
218 plasmon resonance peak centred at around 800 nm. Diameter 38.1 ± 2.8 nm are derived from
219 TEM analysis for gold nanospheres. Diameter 12.7 ± 1.8 nm and length 51.6 ± 8.2 nm are
220 found for gold nanorods. The aspect ratio (long axis divided by diameter) of GNRs is around
221 4. Further PSS and PAH coating were applied to this GNR.

222 **3.2 Effect of nanoparticles on mortality, hatching and heart rate**

To assess the potential toxicity of the nanoparticles, testing was performed in zebrafish embryos at 6hpf to 120hpf. Toxic endpoints such as mortality, hatching, heart rate and abnormalities were observed and recorded. The doses (0.01nM, 0.025nM, 0.05nM and 0.1nM) of nanoparticles were prepared from 0.1nM stock. The toxic end points were observed, recorded and analysed.

Mortality was defined as the percentage of dead zebrafish eggs from the total number of eggs used for the particular test sample. In the control groups at 72 hpf mortality was below 10% in all experiments, therefore the requirement of OECD guidelines (http://www.oecd.org/) for a valid test was always met and the observed effects can be attributed to these nanoparticle samples. Most of the eggs showed coagulation at 24hpf and by 48hpf many of the vital embryos had no heartbeat and were determined as mortal. A few showed developmental retardation and were determined as mortal at 24hpf. Mortality rate is shown in Figure 3. GNRs (CTAB capped) induced a statistically significant increase in mortality at all doses. PSS-GNRs induced a statistically significant increase in mortality only at the high doses. PAH/PSS-GNRs and GNSs caused no significant mortality at all doses tested.

Hatching is defined as the percentage of embryos hatched by the end of the 3rd day from the total number of embryos used for the particular test sample. In the control groups at 72 hpf, the hatching was above 70% in all experiments. Embryos out of their chorion were determined as hatched and the others were termed as unhatched. Hatching rate is shown in Figure 4. Exposure to GNRs and PSS-GNRs caused a statistically significant decrease in hatching at all doses. PAH/PSS-GNRs induced a statistically significant decrease in hatching only at high doses and GNSs had no effect on hatching at all the doses tested.

Heart rate (number of heart-beat per minute) at the end of treatment was observed with a microscope and counted using a cell counter. The heart rate of the nanoparticle-treated

samples was compared with the heart rate of control embryos (E3 medium) at 120hpf. Heart rates are shown in Fig. 5. GNRs and PSS-GNRs induced a statistically significant decrease in the heart rate in zebrafish embryos at the high doses only. PAH/PSS-GNRs and GNSs showed no significant impact on the heart rate at all doses tested.

3.3 Effect of nanoparticles on expression of oxidative stress genes

Oxidative stress represents an imbalance between the production of reactive oxygen species (ROS) and the neutralization of excess ROS by cellular antioxidant defences. Nanoparticles have been demonstrated to cause oxidative stress in different types of cells and animal models including zebrafish (Abdal Dayem *et al*., 2017; Choi *et al*., 2010; Faria *et al*., 2014; Zhao *et al*., 2016). Using qRT-PCR we examined expression of oxidative stress related genes in nanoparticle treated and control zebrafish embryos and found that treatment with GNRs induced significant changes in the expression of all the oxidative stress related genes studied compared to the controls (Fig. 6). PAH-PSS-GNRs induced a significant change only in catalase expression, while treatment with GNSs and PSS-GNRs caused no significant change in the examined genes. The results clearly demonstrate that PSS coating on GNR nanoparticles reduced toxicity, possibly by forming a protective layer around CTAB of GNRs.

3.4 Effect of nanoparticles on apoptosis

Acridine orange staining was performed to detect any apoptosis caused by the nanoparticle treatment (Fig. 7). It is important for a multicellular organism to maintain and regulate cell numbers. One such response to injury or infection is apoptosis. Acridine orange staining works on the principle that healthy cells are not permeable to acridine orange, which can pass through only the damaged cell membrane. Each bright spot represents an area of cell death, with the intensity of fluorescence directly correlated to the extent of apoptosis (Fig. 7A-E).

Apoptosis was seen in all the cases of nanoparticle treatment, although the intensity varied, becoming greater with a rise in nanoparticle concentration (data not shown).

4 DISCUSSION

From the displayed results (Fig. 3, 4, and 5), it can be seen that GNRs (CTAB capped) showed high toxicity when compared to the other types of gold nanoparticles tested. GNRs induced a statistically significant increase in mortality and decrease in hatching percentage at all doses. GNRs also showed a significant decrease in heart rate at high doses. PSS-GNRs induced a statistically significant decrease in hatching rate at all doses and increased mortality and decreased heart rate at high doses. PAH/PSS-GNRs showed a significant decrease in hatching at high doses. GNSs showed no significant toxicity even at the highest dose. This may be due to the shape of the nanoparticle or the surfactant used for the purpose of capping. It is clearly seen that PSS and PAH/PSS-capped GNRs induced less toxic effects when compared to GNRs. The toxic impact of GNRs may be due to CTAB (surfactant). The toxicity of CTAB was investigated by Wang *et al*. (2008) and Alkilany *et al*. (2009). Similar toxic effects of nanoparticles on HEP-2 and MDCK cells were reported by Zhang *et al*., (2012). This difference in toxicity cannot be explained only by the size and shape of the nanoparticle. To account for the difference, two interesting explanations have been proposed. One of them involves the charge on the nanoparticle while the other pertains to the diffusion pathway. In the case of the former, it has been shown that gold nanoparticles which are cationic are more toxic as it is easier for them to be absorbed into the negatively charged cell membrane; in the case of the latter, nanoparticles that are cationic can pass through the cell membrane via the direct diffusion pathway while anionic nanoparticles have to pass through the cell membrane by endocytosis. Given that both GNRs and PAH/PSS-GNRs are cationic while GNSs and PSS-GNRs are anionic, these characteristics in combination with the toxic surfactant (CTAB) may explain the greater toxicity exhibited by GNRs.

297 Nanoparticles can induce oxidative stress in human fibroblasts, erythrocytes, vascular
298 endothelial cells, mesenchymal stem cells and a variety of tumour cells (Abdal Dyem *et al*.,
299 2017). Nanoparticles have also been shown to cause oxidative stress in zebrafish embryos
300 and in the liver of adult zebrafish (Choi *et al*., 2010; Du *et al*., 2017; Faria *et al*., 2014; Zhao
301 *et al*., 2016). Catalase, GPX and SOD are detoxifying enzymes for ROS that regulate redox
302 homeostasis (Abdal Dyem *et al*., 2017). Bcl2 plays an important role in regulation of ROS
303 generation and maintenance of the redox status (Hockenbery *et al*., 1993). Du *et al*. (2017)
304 showed that zinc oxide nanoparticle treatment resulted in significant increases in SOD and
305 GPX activities in zebrafish embryos. Zhao *et al*. (2016) also demonstrated significantly
306 increased SOD activity in zebrafish embryos treated with zinc oxide nanoparticles. We found
307 that GNRs markedly upregulated expression of *Catalase*, *GPX1a*, *Sod1* and *Bcl-2* genes (Fig.
308 6), suggesting that GNR treatment caused oxidative stress and led to antioxidant responses.
309 Nanoparticles have been reported to cause apoptosis in zebrafish embryos and tissues of
310 adult zebrafish (Choi *et al*., 2010; Du *et al*., 2017; Zhao *et al*., 2016). We examined the
311 apoptotic effects of nanoparticle exposure (0.05nM) and found the most common feature
312 being the crowded bright spots in the heart and eye areas (Fig. 7), representing the
313 accumulation of toxic substances ultimately leading to apoptosis. Bcl-2 is considered to be an
314 anti-apoptotic protein that protects cells from apoptosis (Hockenbery *et al*., 1993). The high
315 level of apoptosis observed in GNR-treated embryos (Fig. 7) was accompanied by a
316 significant upregulation of Bcl-2 expression in GNR-treated embryos when compared to
317 untreated control embryos (Fig. 6D), indicating a defensive response to counteract the
318 damaging effects of GNR exposure. A previous study reported that myocyte apoptosis can
319 lead to dilated cardiomyopathy (Wencker *et al*., 2003). Similar results were reported when
320 zebrafish were treated with hexabromocyclododecane (HBCD) and microcystins (MCs).
321 These results suggest that the nanoparticles are primarily targeting the heart area during the

treatment process, which may result in a reduction of heart rate and blood flow and ultimately slowing growth and development (Zeng *et al*., 2014; Ulukaya *et al*., 2011; Deng *et al*., 2009). Similar results were reported by Zhang *et al*., 2012, when nanoparticles were tested on HEP-2 and MDCK cells. Abnormalities were also observed in the higher concentration of each sample. The abnormalities include slimy fluid with brown flakes, abnormal spine, heart oedema, curved tail, and degraded body parts (data not shown).

5 CONCLUSION

GNRS and PSS-GNRS exhibited significant toxic action by increasing mortality and by decreasing hatching and heart rate. The results clearly demonstrate that the GNRs are the most toxic and GNSs the least toxic of all the compared nanoparticles. PSS coating on GNRs nanoparticles reduced toxicity possibly by forming a protective layer around CTAB of GNRs. The addition of an extra layer of PAH on PSS-GNRs further reduced the toxicity. This may be a result of the coating which leads to the further isolation of toxic CTAB from cell membrane and hence a change in toxicity. This might suggest a new way to combat toxicity although further study is required.

ACKNOWLEDGEMENT

This work was supported by the Royal Society, the Rosetrees Trust (M160, M160-F1 and M160-F2), the Glasgow Children's Hospital Charity (YRSS/PSG/2014), and the Visual Research Trust (VR2014). Maintenance of the zebrafish facility was funded by the European Union INTERREG NEW noPILLS programme.

REFERENCES

Abdal Dayem, A., Hossain, M.K., Lee, S.B., Kim, K., Saha, S.K., Yang, G.M., … Cho, S.G. (2017). The role of reactive oxygen species (ROS) in the biological activities of metallic nanoparticles. *International Journal of Molecular Sciences, 18*(1), pii: E120.

Alkilany, A.M., Nagaria, P.K., Hexel, C.R., Shaw, T.J., Murphy, C.J., & Wyatt, M.D (2009). Cellular uptake and cytotoxicity of gold nanorods: molecular origin of cytotoxicity and surface effects. *Small, 5*(6), 701-708.

Asharani, P.V., Low Kah Mun, G., Hande, M.P., & Valiyaveettil, S. (2008). Cytotoxicity and genotoxicity of silver nanoparticles in human cells. *ACS Nano*, *3*(2), 279-290.

Asharani, P.V., Wu, Y.L., Gong, Z., & Valiyaveettil, S. (2008). Toxicity of silver nanoparticles in zebrafish models. *Nanotechnology*, *19*(25), 255102.

Bar-Ilan, O., Albrecht, R. M., Fako, V. E., & Furgeson, D. Y. (2009). Toxicity assessments of multisized gold and silver nanoparticles in zebrafish embryos. *Small*, 5(16), 1897-1910.

Cattaneo, A. G., Gornati, R., Bernardini, G., Sabbioni, E., Manzo, L., & Di Gioacchino, M. (2014). Testing nanotoxicity: an update of new and traditional methods. Handbook of Nanotoxicology, Nanomedicine and Stem Cell Use in Toxicology, 3-34.

Choi, J.E., Kim, S., Ahn, J.H., Youn, P., Kang, J.S., Park, K., … Ryu, D.Y. (2010). Induction of oxidative stress and apoptosis by silver nanoparticles in the liver of adult zebrafish. *Aquatic Toxicology*, *100*, 151-159.

Deng, J., Yu, L., Liu, C., Yu, K., Shi, X., Yeung, L.W., … Zhou, B. (2009). Hexabromocyclododecane-induced developmental toxicity and apoptosis in zebrafish embryos. *Aquatic Toxicology*, *93*(1), 29-36.

Du, J., Cai, J., Wang, S., & You, H. (2017). Oxidative stress and apotosis to zebrafish (Danio rerio) embryos exposed to perfluorooctane sulfonate (PFOS) and ZnO nanoparticles. *International Journal of Occupational Medicine and Environmental Health*, *30*(2), 213-229.

370 Faria, M., Navas, J.M., Ráldua, D., Soares, A.M., & Barata, C. (2014). Oxidative stress
371 effects of titanium dioxide nanoparticle aggregates in zebrafish embryos. *Science of the Total*
372 *Environment*, *470-471*, 379-389.
373 Gu, A.H., Shi, X.G., Yuan, C., Ji, G.C., Zhou, Y., Long, Y., … Wang, X.R. (2010).
374 Exposure to fenvalerate causes brain impairment during zebrafish development.
375 *Toxicology Letters*, *197*, 188-192.
376 Hanley, C., Thurber, A., Hanna, C., Punnoose, A., Zhang, J., & Wingett, D.G. (2009).
377 The influences of cell type and ZnO nanoparticle size on immune cell cytotoxicity and
378 cytokine induction. *Nanoscale research letters*, *4*(12), 1409.
379 Hockenbery, D.M., Oltvai, Z.N., Yin, X.M., Milliman, C.L., Korsmeyer, S.J. (1993). Bcl-2
380 functions in an antioxidant pathway to prevent apoptosis. Cell, 75(2), 241-251.
381 Jiang, J.Q., Zhou, Z., Patibandla, S., & Shu, X. (2013). Pharmaceutical removal from
382 wastewater by ferrate (VI) and preliminary effluent toxicity assessments by the zebrafish
383 embryo model. *Microchemical Journal*, *110*, 239-245.
384 Kimling, J., Maier, M., Okenve, B., Kotaidis, V. Ballot, H., & Plech, A. (2006). Turkevich
385 method for gold nanoparticle synthesis revisited. *Journal of Physical Chemistry B*, *109*,
386 15700-15707.
387 Marambio-Jones, C., & Hoek, E. M. V. (2010). A review of the antibacterial effects of silver
388 nanomaterials and potential implications for human health and the environment. *Journal of*
389 *Nanoparticle Research*, *12*(5), 1531− 1551.
390 Murphy, C.J. & Jana, N.R. (2002). Controlling the aspect ratio of inorganic nanorods and
391 nanowires. *Advanced Materials*, *14*(1), 80-82.
392 Omura, N., Uechi, I., & Yamada, S. (2009). Comparison of plasmonic sensing between
393 polymer- and silica-coated gold nanorods. *Analytical Sciences*, *25*(2), 255-259.

Raghupathy, R.K., Gautier, P., Soares, D.C., Wright, A.F., & Shu, X. (2015). Evolutionary Characterization of the retinitis pigmentosa GTPase regulator gene. *Investigative Ophthalmology and Visual Science*, *56*(11):6255-6264.

Salata, O. V. (2004) Applications of nanoparticles in biology and medicine. *Journal of Nanobiotechnology*, *2*(1), 3.

Shu, X., Zeng, Z., Gautier, P., Lennon, A., Gakovic, M., Patton, E.E., & Wright, A.F. (2010). Zebrafish Rpgr is required for normal retinal development and plays a role in dynein-based retrograde transport processes. *Human Molecular Genetics*, *19*(4), 657-670.

Si, J., Zhang, H., Wang, Z., Wu, Z., Lu, J., Di, C., … Wang X. (2013). Effects of 12C 6+ ion radiation and ferulic acid on the zebrafish (Danio rerio) embryonic oxidative stress response and gene expression. *Mutation Research*, *745-746*, 26-33.

Ulukaya, E., Acilan, C., & Yilmaz, Y. (2011). Apoptosis: why and how does it occur in biology? *Cell Biochemistry and Function*, *29*(6), 468-480.

Wencker, D., Chandra, M., Nguyen, K., Miao, W., Garantziotis, S., Factor, S.M., & Kitsis, R.N. (2003). A mechanistic role for cardiac myocyte apoptosis in heart failure. *Journal of Clinical Investigation*, *111*(10), 1497-1504.

Wang, S., Lu, W., Tovmachenko, O., Rai, U.S., Yu, H., & Ray, P.C. (2008). Challenge in understanding size and shape dependent toxicity of gold nanomaterials in human skin keratinocytes. *Chemical Physics Letters*, *463*(1), 145-149.

Wei, G., Simionesie, D., Sefcik, J., Sutter, J. U., Xue, Q., Yu, J., … Chen, Y. (2015). Revealing the photophysics of gold-Nanobeacons via time-resolved fluorescence spectroscopy. *Optics Letters*, *40*, 5738-5741.

Wei, G., Yu, J., Wang, J., Gu, P., Birch, D.J.S., & Chen, Y. (2016). Hairpin DNA-functionalized gold nanorods for mRNA detection in homogenours solution. *Journal of Biomedical Optics*, *21*(9), 97001.

Wolf, K., Stafoggia, M., Cesaroni, G., Andersen, Z.J., Beelen, R., Galassi, C., … Forastiere, F. (2015). Long-term Exposure to Particulate Matter Constituents and the Incidence of Coronary Events in 11 European Cohorts. *Epidemiology*, *26*(4), 565-574.

Zhang, Y., Yu, j., Birch, D. J., & Chen, Y. (2010). Gold nanorods for fluorescence lifetime imaging in biology. *Journal of Biomedical Optics*, *15*, 20504.

Zhang, Y., Birch, D.J.S., & Chen, Y. (2011). Two-photon excited surface plasmon enhanced energy transfer between DAPI and gold nanoparticles: Opportunities in intra-cellular imaging and sensing. *Applied Physics Letters*, *99*, 103701.

Zhang, Y., Xu, D., Li, W., Yu, J., & Chen, Y. (2012) Effect of size, shape, and surface modification on cytotoxicity of gold nanoparticles to human HEp-2 and canine MDCK cells. *Journal of Nanomaterials*, *2012*, ID 375496.

Zhang, Y., Wei, G., Yu, J., Birch, D. J. S., & Chen Y. (2015). Surface plasmon enhanced energy transfer between gold nanorods and fluorophores: application to endocytosis study and RNA detection. *Faraday Discuss*, *178*, 383-394

Zeng, C., Sun, H., Xie, P., Wang, J., Zhang, G., Chen, N., … Li, G. (2014). The role of apoptosis in MCLR-induced developmental toxicity in zebrafish embryos. *Aquatic Toxicology*, *149*, 25-32.

Zhao, X., Ren, X., Zhu, R., Luo, Z., & Ren, B. (2016). Zinc oxide nanoparticles induce oxidative DNA damage and ROS-triggered mitochondria-mediated apoptosis in zebrafish embryos. *Aquatic Toxicology*, *180*, 56-70.

Table 1: Primers used in qRT-PCR.

Gene name	Primer sequence	Reference
Gpx1a	Forward: ACCTGTCCGCGAAACTATTG Reverse: TGACTGTTGTGCCTCAAAGC	Choi JE et al., 2010
Catalase	Forward: AGGGCAACTGGGATCTTACA Reverse: TTTATGGGACCAGACCTTGG	Choi JE et al., 2010
Sod1	Forward: GTCGTCTGGCTTGTGGAGTG Reverse : TGTCAGCGGGCTAGTGCTT	Si J et al., 2013
Bcl-2	Forward: AGGAAAATGGAGGTTGGGATG Reverse : TGTTAGGTATGAAAACGGGTGG	Si J et al., 2013
18S RNA	Forward : CCACTCCCGAGATCAACTA Reverse : CAAATTACCCATTCCCGACA	Raghupathy R et al., 2015

Figure legends:

Figure 1 Absorption spectra for GNRs, PSS-GNRs and GNSs

Figure 2 Transmission electric microscopy (TEM) images of gold nanospheres (A) and gold nanorods (B)**.**

Figure 3 Mortality of zebrafish embryos following 120 hpf treatments with different concentrations of different nanoparticles. Eight embryos were used for each treatment. Significant increases in mortality rate relative to that of control fish were observed following exposure to all concentrations of GNRs and to 0.05 and 0.1nM PSS-GNRs. (***p<0.001; ** p<0.01; *p<0.05). Values are expressed as mean ± standard deviation.

Figure 4 Hatching rate of zebrafish embryos following 72 hpf treatments with different concentrations of different nanoparticles. Eight embryos were used for each treatment. Significant decreases in hatching rate relative to that of control fish were observed following exposure to all concentrations of GNRs and PSS-GNRs and to 0.05 and 0.1nM PSS/PSH-GNRs (****p<0.0001; *** p<0.001; **p<0.01; *p<0.05). Values are expressed as mean ± standard deviation.

Figure 5 Heart rate (beats per minute) of zebrafish embryos following 120 hpf treatments with different concentrations of different nanoparticles. Significant differences in heart rate relative to that of control fish were observed following exposure to 0.05 and 0.1nM GNRs and to 0.1nM PSS-GNRs (****p<0.0001; *** p<0.001; * p<0.05). Values are expressed as mean ± standard deviation.

Figure 6 Expression of oxidative stress genes in zebrafish embryos treated with nanoparticles (2.5 μM GNS, 0.01 nM GNR, 0.025 nM PSS-GNR and 0.05 nM PAH/PSS-GNR) from 6 hpf to 72 hpf. (A) Catalase, (B) Gpx1a, (C) Sod1, (D) Bcl-2. Significant differences in gene expression relative to that in control fish are indicated by asterisks (***p<0.001 and ** p<0.01). Data were presented as mean ± standard deviation.

Figure 7 Acridine orange staining of zebrafish embryos (48 hpf) treated with 0.05nM concentration of nanoparticles. (A) GNRs, (B) GNSs, (C) PSS-GNRs, (D) PSS/PSH-GNRs, (E) Control. (F)The bright green spots indicate the presence of apoptotic cells. The fluorescent signals were quantified using ImageJ, the relative fluorescent signals in treated zebrafish embryos were significantly higher than that of control embryos. GNRs-treated embryos had highest fluorescent signals. ****p<0.0001.

Figure 1

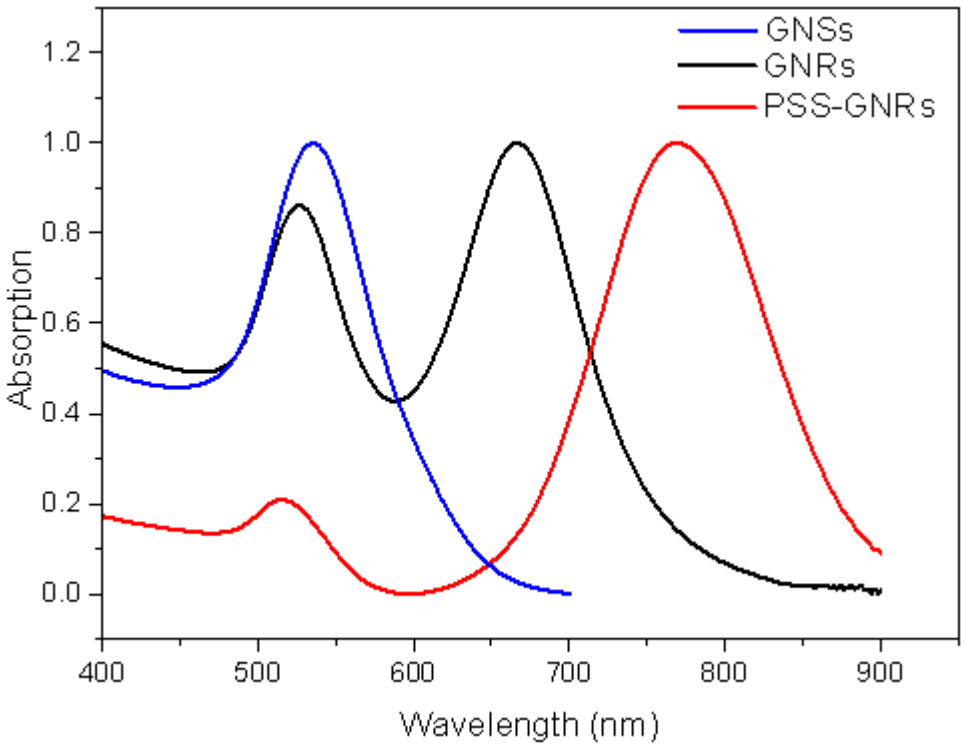

Figure 2

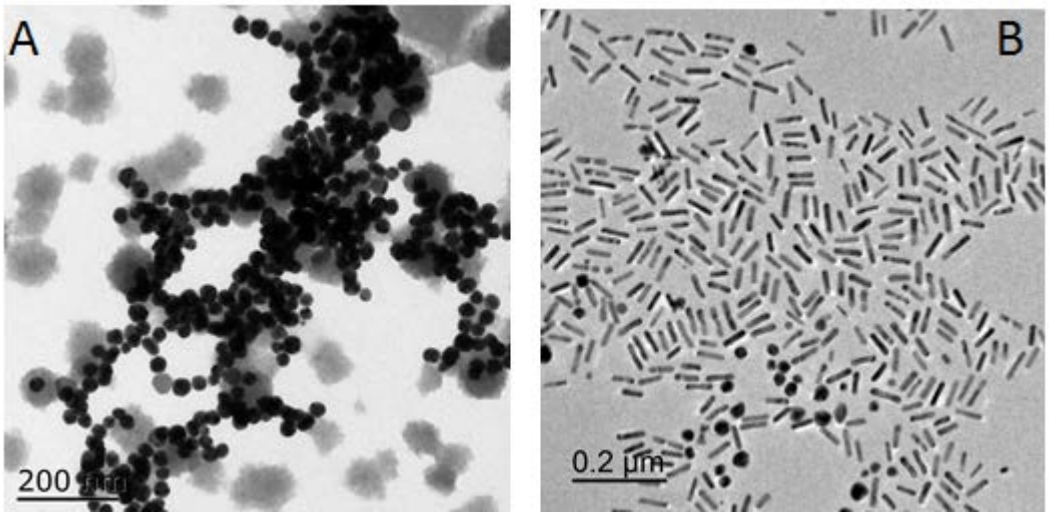

Figure 3

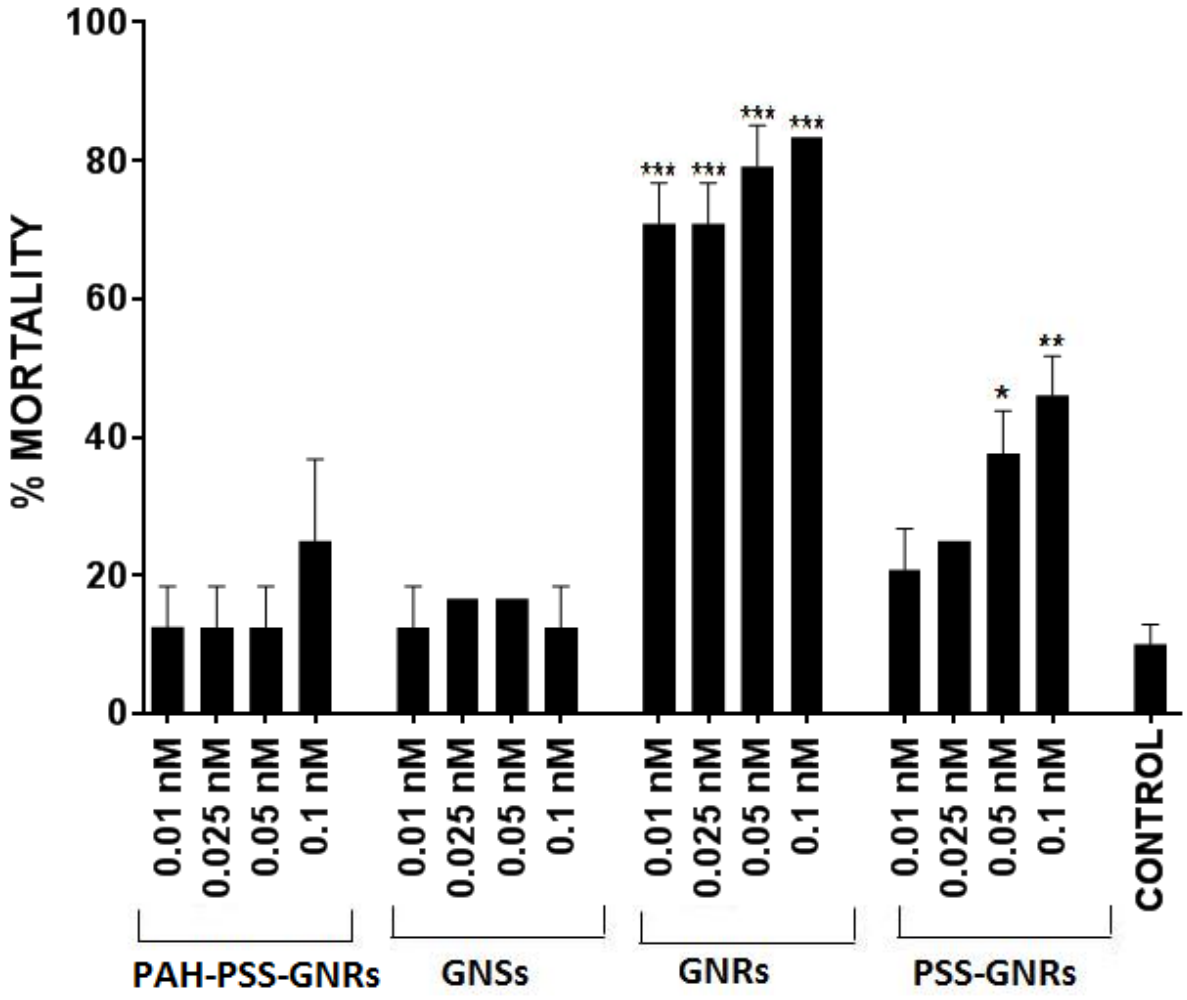
100
80
60
40
20
0
% MORTALITY
***
***
***
***
*
**
0.01 nM
0.025 nM
0.05 nM
0.1 nM
0.01 nM
0.025 nM
0.05 nM
0.1 nM
0.01 nM
0.025 nM
0.05 nM
0.1 nM
0.01 nM
0.025 nM
0.05 nM
0.1 nM
CONTROL
PAH-PSS-GNRs
GNSs
GNRs
PSS-GNRs

Figure 4

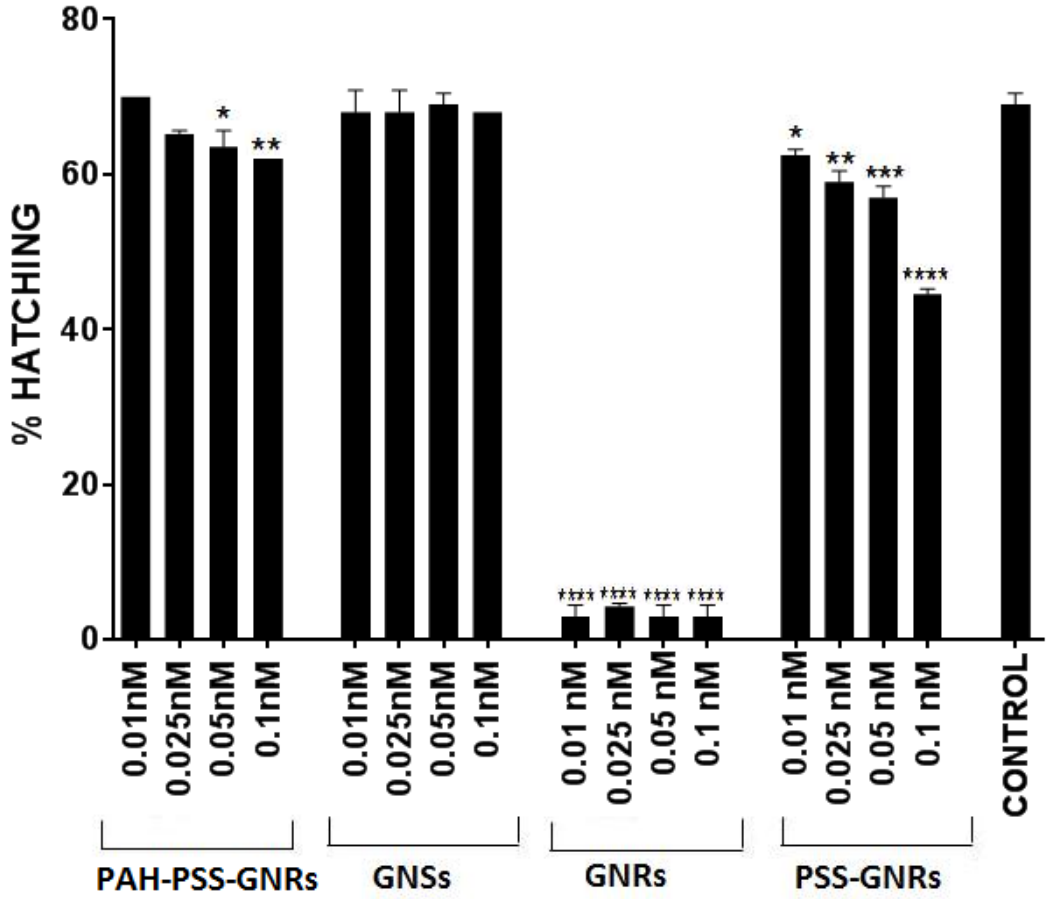
80
60
40
20
0
% HATCHING
*
**
*
**
***
****
0.01nM
0.025nM
0.05nM
0.1nM
0.01nM
0.025nM
0.05nM
0.1nM
0.01 nM
0.025 nM
0.05 nM
0.1 nM
0.01 nM
0.025 nM
0.05 nM
0.1 nM
CONTROL
PAH-PSS-GNRs
GNSs
GNRs
PSS-GNRs

Figure 5

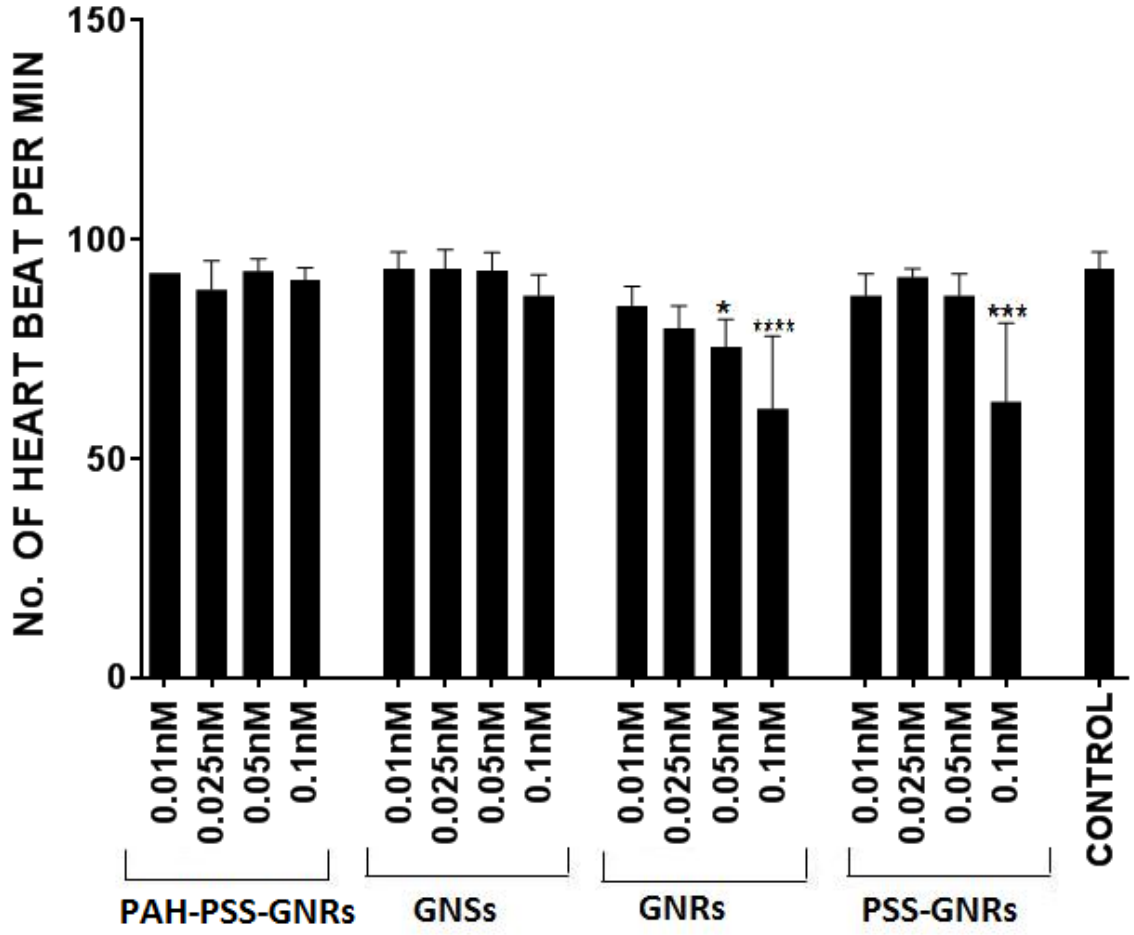
No. OF HEART BEAT PER MIN
150
100
50
0
*
****
***
0.01nM
0.025nM
0.05nM
0.1nM
0.01nM
0.025nM
0.05nM
0.1nM
0.01nM
0.025nM
0.05nM
0.1nM
0.01nM
0.025nM
0.05nM
0.1nM
CONTROL
PAH-PSS-GNRs
GNSs
GNRs
PSS-GNRs

Figure 6

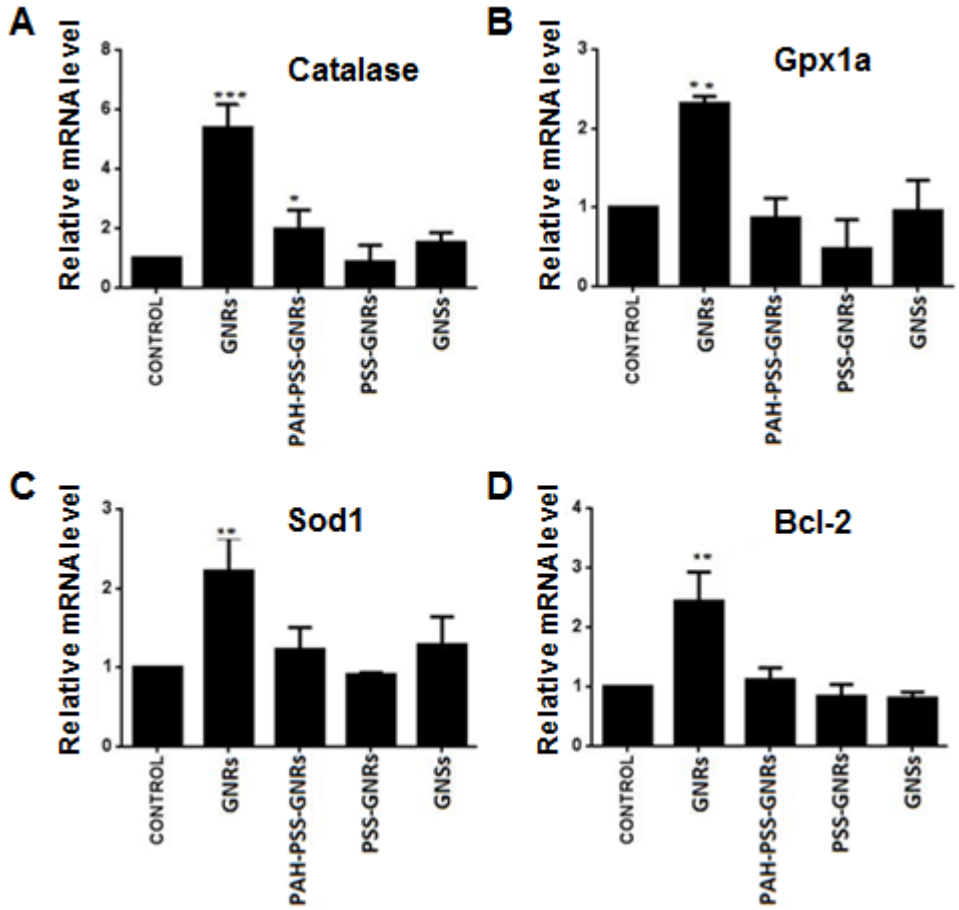
A
Catalase
Relative mRNA level
CONTROL
GNRs
PAH-PSS-GNRs
PSS-GNRs
GNSs
B
Gpx1a
Relative mRNA level
C
Sod1
Relative mRNA level
D
Bcl-2
Relative mRNA level

559 **Figure 7**

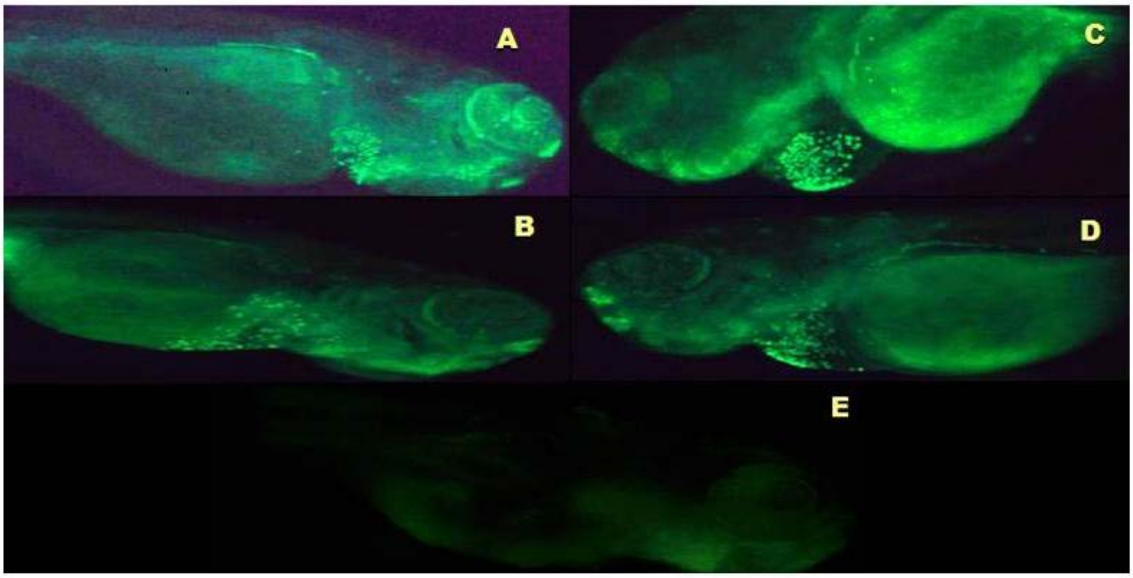

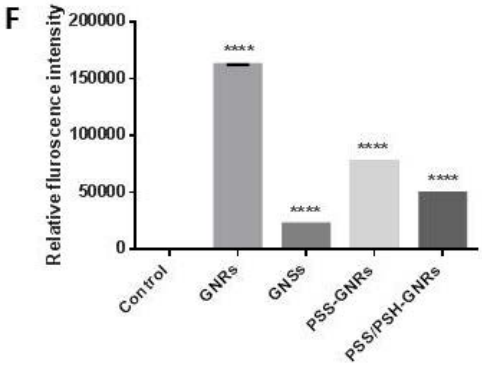

560

561